The Zds proteins control entry into mitosis and target protein phosphatase 2A to the Cdc25 phosphatase

Sidonie Wicky[a,*], Hendri Tjandra[a,†], David Schieltz[b], John Yates III[b], and Douglas R. Kellogg[a]

[a]Department of Molecular, Cell, and Developmental Biology, University of California, Santa Cruz, CA 95064; and
[b]Department of Chemical Physiology, The Scripps Research Institute, La Jolla, CA 92037

ABSTRACT **The Wee1 kinase restrains entry into mitosis by phosphorylating and inhibiting cyclin-dependent kinase 1 (Cdk1). The Cdc25 phosphatase promotes entry into mitosis by removing Cdk1 inhibitory phosphorylation. Experiments in diverse systems have established that Wee1 and Cdc25 are regulated by protein phosphatase 2A (PP2A), but a full understanding of the function and regulation of PP2A in entry into mitosis has remained elusive. In budding yeast, entry into mitosis is controlled by a specific form of PP2A that is associated with the Cdc55 regulatory subunit ($PP2A^{Cdc55}$). We show here that related proteins called Zds1 and Zds2 form a tight stoichiometric complex with $PP2A^{Cdc55}$ and target its activity to Cdc25 but not to Wee1. Conditional inactivation of the Zds proteins revealed that their function is required primarily at entry into mitosis. In addition, Zds1 undergoes cell cycle–dependent changes in phosphorylation. Together, these observations define a role for the Zds proteins in controlling specific functions of $PP2A^{Cdc55}$ and suggest that upstream signals that regulate $PP2A^{Cdc55}$ may play an important role in controlling entry into mitosis.**

Monitoring Editor
David G. Drubin
University of California, Berkeley

Received: Jun 7, 2010
Revised: Nov 5, 2010
Accepted: Nov 10, 2010

INTRODUCTION

Mitosis is initiated by synthesis of mitotic cyclins, which bind and activate cyclin-dependent kinase 1 (Cdk1) (Morgan, 2007). The Wee1 kinase inhibits Cdk1 via phosphorylation of a conserved tyrosine, which restrains entry into mitosis (Nurse, 1975; Nurse *et al.*, 1976; Russell and Nurse, 1987). The Cdc25 phosphatase promotes entry into mitosis by removing the inhibitory phosphate (Russell and Nurse, 1986; Gautier *et al.*, 1991; Kumagai and Dunphy, 1991). In both fission yeast and budding yeast, Wee1 mutants cause premature mitosis at a reduced cell size, whereas Cdc25 mutants cause delayed mitosis and increased cell size (Nurse, 1975; Fantes and Nurse, 1977; Russell and Nurse, 1986; Russell *et al.*, 1989; Rupes *et al.*, 2001; Jorgensen *et al.*, 2002; Rupes, 2002; Harvey and Kellogg, 2003; Kellogg, 2003; Harvey *et al.*, 2005; Pal *et al.*, 2008; Rahal and Amon, 2008). These observations led to the hypothesis that Wee1 and Cdc25 mediate a cell size checkpoint that delays mitosis until a critical size has been reached. It also has been proposed that Wee1 and Cdc25 monitor the status of the actin cytoskeleton to link entry into mitosis to cellular morphogenesis (Lew and Reed, 1995; McMillan *et al.*, 1998; Gachet *et al.*, 2001; Lew, 2003). It has been difficult, however, to unambiguously define the cellular events that are monitored by Wee1 and Cdc25 because the upstream signals that control their activity are poorly understood. Elucidation of these signals is therefore an essential step toward understanding entry into mitosis.

Cdk1 is an important regulator of Wee1. The budding yeast Wee1 homologue is referred to as Swe1. Mitotic Cdk1 directly phosphorylates Swe1 on multiple Cdk1 consensus sites, which activates Swe1 to bind, phosphorylate, and inhibit Cdk1 (Harvey *et al.*, 2005). Cdk1 also activates Wee1 in human cells, which suggests that this mechanism is conserved (Deibler and Kirschner, 2010). The initial activating phosphorylation of Swe1 by Cdk1 is followed by further phosphorylation events that lead to full hyperphosphorylation of

This article was published online ahead of print in MBoC in Press (http://www.molbiolcell.org/cgi/doi/10.1091/mbc.E10-06-0487) on November 30, 2010.

*Present address: Toby Robins Breakthrough Breast Cancer Centre, Institute of Cancer Research, 237 Fulham Road, Chelsea, London, SW3 6JB, UK.

†Present address: Global Biological Development, Bayer Healthcare, 800 Dwight Way, Berkeley, CA 94710.

Address correspondence to: Douglas R. Kellogg (dkellogg@ucsc.edu).

Abbreviations used: Cdk1, cyclin-dependent kinase 1; DMSO, dimethyl sulfoxide; DTT, dithiothreitol; PBS, phosphate-buffered saline; PMSF, phenylmethylsulfonyl fluoride; PP2A, protein phosphatase 2A; YPD, yeast extract–peptone–dextrose.

Wee1 (Harvey *et al.*, 2005). In yeast and vertebrates, it appears that mitotic Cdk1, when present at sufficiently high levels, can fully hyperphosphorylate and inactivate Wee1 family members (Tang *et al.*, 1993; Mueller *et al.*, 1995; Harvey *et al.*, 2005). However, multiple kinases are required for full hyperphosphorylation of Wee1 family members in vivo, and their relative contributions are unclear (Wu and Russell, 1993; Mueller *et al.*, 1995; Shulewitz *et al.*, 1999; Sreenivasan and Kellogg, 1999; Asano *et al.*, 2005). Phosphorylation of Xenopus Wee1 is further controlled by protein phosphatase 2A (PP2A), although the role played by PP2A is unknown (Tang *et al.*, 1993).

Cdk1 is also an important regulator of Cdc25. In Xenopus, Cdk1 directly phosphorylates Cdc25, which stimulates a basal interphase activity of Cdc25 approximately fivefold (Izumi *et al.*, 1992; Kumagai and Dunphy, 1992; Hoffman *et al.*, 1993; Izumi and Maller, 1993). Cdk1-dependent inhibition of Wee1 and activation of Cdc25 are thought to constitute feedback loops that promote activation of Cdk1; however, the mechanisms that trigger the feedback loops are poorly understood. An oft proposed model is that the feedback loops are initiated by signals that stimulate Cdc25, and recent experimental evidence supports a model in which Cdc25 plays a crucial role in triggering full activation of Cdk1 (Deibler and Kirschner, 2010). However, the signals that control Cdc25 in this context are poorly understood. Phosphorylation of Xenopus Cdc25 is controlled by PP2A, yet the precise role of PP2A is unknown (Healy *et al.*, 1991; Izumi *et al.*, 1992; Kumagai and Dunphy, 1992; Clarke *et al.*, 1993; Izumi and Maller, 1995; Zhao *et al.*, 1997; Castilho *et al.*, 2009; Mochida *et al.*, 2009). It also appears that a kinase other than Cdk1 can phosphorylate Cdc25 in interphase, but the identity of the kinase is unknown (Kumagai and Dunphy, 1992; Izumi and Maller, 1995). In vertebrates and fission yeast, DNA damage checkpoint signals control Cdc25 via the Chk1 kinase and the PP1 phosphatase (Perry and Kornbluth, 2007; Wang *et al.*, 2008; Reinhardt and Yaffe, 2009).

The budding yeast homologue of Cdc25, referred to as Mih1, is extensively hyperphosphorylated during interphase and undergoes dephosphorylation during entry into mitosis. The bulk of the hyperphosphorylation that occurs during interphase is dependent on casein kinase 1, which is encoded by a pair of redundant genes called *YCK1* and *YCK2* (Robinson *et al.*, 1992, 1993; Pal *et al.*, 2008). Loss of Yck1/2 causes defects in regulation of Cdk1 inhibitory phosphorylation; however, it is unclear whether Yck1/2 play a positive or negative role in regulation of Mih1 because they may also regulate Swe1 (Pal *et al.*, 2008). It is also unclear whether Yck1/2 phosphorylate Mih1 directly because thus far they have been found to phosphorylate Mih1 only weakly in vitro (Pal *et al.*, 2008). Mih1 is phosphorylated by Cdk1 during mitosis and may therefore be subject to positive feedback, as proposed for vertebrate Cdc25 (Pal *et al.*, 2008). The dephosphorylation of Mih1 that occurs as cells enter mitosis is dependent on $PP2A^{Cdc55}$ (Pal *et al.*, 2008). Inactivation of $PP2A^{Cdc55}$ causes increased Cdk1 inhibitory phosphorylation and a prolonged delay in entry into mitosis (Minshull *et al.*, 1996; Yang *et al.*, 2000; Pal *et al.*, 2008). Similarly, inactivation of $PP2A^{Cdc55}$ catalytic subunits after cells have passed through the S phase causes delayed entry into mitosis and severe defects in activation of mitotic Cdk1 (Lin and Arndt, 1995). The phenotypes caused by *cdc55*Δ are largely rescued by *swe1*Δ or by a mutant version of Cdk1 that can not be inhibited by Swe1. These observations demonstrate that a key function of $PP2A^{Cdc55}$ is to regulate Cdk1 inhibitory phosphorylation (Lin and Arndt, 1995; Yang *et al.*, 2000; Pal *et al.*, 2008).

In summary, there has been significant progress toward elucidating the mechanisms that regulate Wee1 and Cdc25 family members, but we still lack a full understanding of the sequence of events that triggers removal of Cdk1 inhibitory phosphorylation and entry into mitosis. Key questions remain unanswered: How are the feedback loops that activate Cdc25 and inactivate Wee1 initiated? How is regulation of Wee1 and Cdc25 linked to upstream checkpoint signals? How are Cdc25 family members activated during entry into mitosis? What is the role of PP2A in entry into mitosis?

To gain new insight into the upstream signals that control entry into mitosis via Wee1 and Cdc25 family members, we characterized the budding yeast Zds1 and Zds2 proteins. Previous work found that Zds1 and Zds2 are required for normal control of Cdk1 inhibitory phosphorylation, but the underlying mechanisms were unknown. Zds1 and Zds2 are redundant paralogues: Loss of either protein does not cause a severe phenotype, but cells lacking both are barely viable, show a prolonged delay at the G2/M transition, and become highly elongated (Bi and Pringle, 1996; Yu *et al.*, 1996). These phenotypes are rescued by *swe1*Δ, which indicates that they are caused by increased Cdk1 inhibitory phosphorylation (Ma *et al.*, 1996; McMillan *et al.*, 1999). The elongated cell phenotype observed in mutants that cause increased Cdk1 inhibitory phosphorylation is due to the fact that mitotic Cdk1 is required for repression of polar bud growth (Surana *et al.*, 1991; Fitch *et al.*, 1992). Two general models could explain the role of Zds1/2 in controlling Cdk1 inhibitory phosphorylation. They may be required for execution of events that occur early in the cell cycle that are monitored by a Swe1-dependent checkpoint. Alternatively, Zds1/2 could play a more direct role in controlling the activity of Swe1 or Mih1, perhaps serving to relay checkpoint signals that determine when it is appropriate to enter mitosis. To help distinguish these models, we analyzed the function and regulation of Zds1/2 during the cell cycle, with the goal of defining how they control Cdk1 inhibitory phosphorylation.

RESULTS

Zds1 and Zds2 execute a function required for normal passage through mitosis

Phenotypes observed previously in *zds1*Δ *zds2*Δ cells suggested that Zds1/2 play a role in mitosis (Bi and Pringle, 1996; Yu *et al.*, 1996; Queralt and Uhlmann, 2008). However, *zds1*Δ *zds2*Δ cells have severe cell-cycle defects, are difficult to synchronize, and rapidly accumulate suppressors. These factors have made it difficult to determine the primary and immediate effects caused by inactivation of Zds1/2. We therefore generated temperature-sensitive alleles of *ZDS1* in a *zds2*Δ background. Seven mutants were isolated that showed a reduced growth rate and an elongated bud phenotype at 37°C. One of the mutants exhibited a growth defect at 34°C (*zds1–1 zds2*Δ), which allowed us to inactivate Zds1/2 without the transient nonspecific heat shock effects that can be caused by a shift to 37°C (Figure 1A). Observation of *zds1–1 zds2*Δ cells shifted to 34°C revealed bud growth defects within 30 min, which indicated rapid inactivation of Zds1 (Figure 1B). The first defect that could be detected at 30 min was a slight elongation of large buds (arrows, Figure 1B). Prolonged incubation at the nonpermissive temperature caused all *zds1–1 zds2*Δ cells to grow highly elongated buds (Figure 1B). This kind of excessive polar growth can be caused by a failure to properly remove Cdk1 inhibitory phosphorylation, because activation of mitotic Cdk1 is required for repression of polar growth (Fitch *et al.*, 1992; Booher *et al.*, 1993; Lew and Reed, 1993; Ma *et al.*, 1996; Sreenivasan and Kellogg, 1999; Longtine *et al.*, 2000). To test whether inactivation of Zds1/2 causes increased Cdk1 inhibitory phosphorylation, we used a phosphospecific antibody to assay Cdk1 inhibitory phosphorylation in synchronized *zds1–1 zds2*Δ and *zds2*Δ control cells. In the control cells, Cdk1 inhibitory phosphorylation peaked at 75 min and then began to decline, whereas in the mutant cells

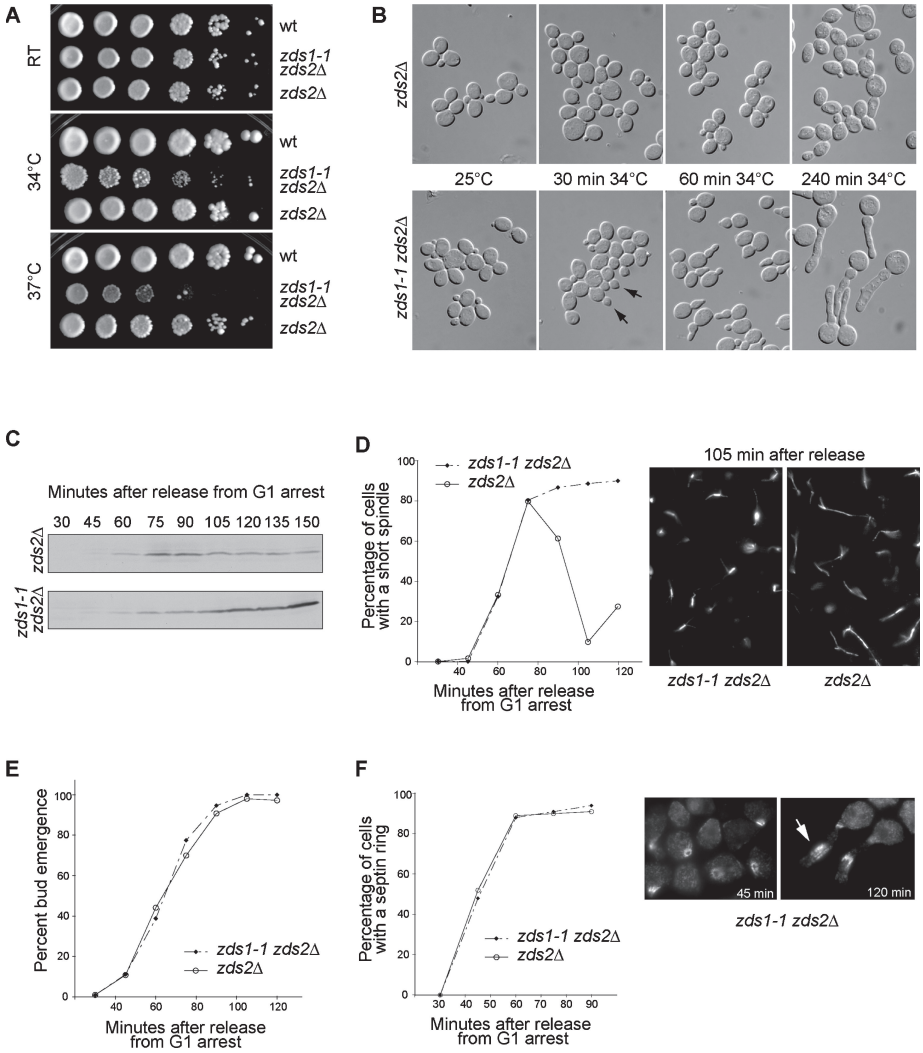

FIGURE 1: Conditional inactivation of Zds1/2 causes defects in mitotic progression. (A) Growth of wild type (wt), *zds1–1 zds2*Δ, and *zds2*Δ control cells was monitored on YPD plates at room temperature (RT), 34°C, and 37°C. (B) Rapidly growing cultures of *zds1–1 zds2*Δ and *zds2*Δ control cells were shifted from 25°C to 34°C for the indicated times. Arrowheads indicate buds with abnormal morphology. (C) *zds1–1 zds2*Δ and *zds2*Δ cells were synchronized in G1 with α-factor at 25°C and released into fresh YPD medium at 34°C. Cells were harvested at the indicated times, and samples were probed with a phosphospecific antibody that recognizes Cdk1 inhibitory phosphorylation. (D) *zds1–1 zds2*Δ and *zds2*Δ cells were synchronized in G1 with α-factor at 25°C and released into fresh YPD medium at 34°C. Cells were harvested at the indicated times, fixed, and stained with an anti-tubulin antibody. The percentage of cells with short spindles was determined at each time point, and images of mitotic spindles were obtained 105 min after release. (E) Bud emergence was assayed in the same cells as in (D). (F) *zds1–1 zds2*Δ and *zds2*Δ cells were handled as in (D), but were stained with an anti-Cdc11 antibody to assay septin ring formation and structure. Images of septin rings in *zds1–1 zds2*Δ were taken at the indicated times after release. At least 200 cells were analyzed for each time point in (D), (E), and (F).

Cdk1 inhibitory phosphorylation increased throughout the time course (Figure 1C). We also found that the slow growth and elongated cell phenotypes caused by the *zds1–1* mutant were rescued by *swe1*Δ, which demonstrated that these defects were due to misregulation of Swe1, Mih1, or both (data not shown). These observations are consistent with previous work that found that the slow growth and elongated cell phenotypes caused by *zds1*Δ *zds2*Δ are rescued by *swe1*Δ (McMillan *et al.*, 1999).

To further characterize the function of Zds1/2 in cell-cycle progression, we analyzed the timing of mitotic spindle formation in synchronized *zds1–1 zds2*Δ cells that were released from a G1 arrest at the restrictive temperature. Short mitotic spindles are formed in early mitosis and require a low level of mitotic Cdk1 activity, whereas long spindles are generated during nuclear division (Fitch *et al.*, 1992; Rahal and Amon, 2008). The timing of short spindle assembly was normal in *zds1–1 zds2*Δ cells; however, the cells underwent a prolonged delay at the short spindle stage (Figure 1D). Previous work found that activation of a Swe1-dependent checkpoint arrest causes cells to undergo a prolonged delay at the short spindle stage of early mitosis (Carroll *et al.*, 1998; Sreenivasan and Kellogg, 1999; Theesfeld *et al.*, 1999). Thus, this result is consistent with the idea that Zds1/2 are required for execution of events that are monitored by the Swe1-dependent checkpoint or that they are responsible for relaying signals that release inhibition of Cdk1 when checkpoint conditions have been satisfied.

To test whether Zds1/2 carry out functions earlier in the cell cycle, we assayed the timing of bud emergence and septin ring formation, both of which occur in the G1 phase. Inactivation of *zds1–1* had no effect on either the timing of bud emergence or the formation of the septin ring (Figure 1, E and F, respectively). The structure of the newly formed septin ring appeared to be normal in the absence of Zds1 function, although we can not rule out the possibility that there are more subtle defects in septin organization that could not be detected by immunofluorescence (Figure 1F, panel labeled 45 min). Abnormal septin structures appeared along the elongated buds after cells arrested in mitosis (Figure 1F, panel labeled 120 min, arrow indicates abnormal septin structure). Similar abnormal septin structures have been observed in cells lacking proteins required for normal regulation of Cdk1 inhibitory phosphorylation (Sreenivasan and Kellogg, 1999; Longtine *et al.*, 2000).

To further define a role for Zds1/2 in control of Cdk1 inhibitory phosphorylation, we tested for genetic interactions between *zds1*Δ and deletions of genes that encode kinases known to be required for normal control of Cdk1 inhibitory phosphorylation, including *CLA4*, *GIN4*, and *ELM1*. Loss of any of these kinases causes a Swe1-dependent G2/M delay and growth of elongated buds (Sreenivasan and Kellogg, 1999; Longtine *et al.*, 2000). We were unable to recover *zds1*Δ *cla4*Δ from crosses, which suggests that they are synthetically lethal. Moreover, *zds1*Δ *gin4*Δ and *zds1*Δ *elm1*Δ cells grew more poorly than either single deletion (data not shown).

Together, these results demonstrate that Zds1/2 execute functions required for normal regulation of Cdk1 inhibitory phosphorylation at G2/M.

Zds1 forms a tight stoichiometric complex with PP2A^{Cdc55}

Zds1/2 were previously found to associate with PP2A in coimmunoprecipitation assays (Gavin *et al.*, 2002; Collins *et al.*, 2007; Queralt and Uhlmann, 2008; Yasutis *et al.*, 2010). Canonical PP2A is a trimeric complex composed of a catalytic subunit, a scaffolding subunit, and a regulatory subunit (Janssens and Goris, 2001; Trinkle-Mulcahy and Lamond, 2006). In budding yeast, the catalytic subunit is encoded by a pair of redundant genes called *PPH21* and *PPH22*, and the scaffolding subunit is encoded by the *TPD3* gene. There are two main regulatory subunits called Cdc55 and Rts1 that associate with PP2A to form distinct complexes referred to as PP2A^{Cdc55} and PP2A^{Rts1}, which perform different functions within the cell (Zhao *et al.*, 1997; Gentry and Hallberg, 2002).

Although Zds1/2 were found to coprecipitate with components of PP2A^{Cdc55}, it was unknown whether they interact with PP2A directly or via additional accessory proteins. It was also unknown whether they interact with multiple PP2A regulatory subunits. To learn more about the association of Zds1/2 with PP2A, we purified Zds1 complexes from yeast. The endogenous copy of Zds1 was tagged with three copies of the influenza hemagglutinin (HA) epitope and placed under the control of the *GAL1* promoter. 3XHA-Zds1 complexes were purified by large-scale immunoaffinity chromatography using anti-HA antibodies and peptide elution. We found three proteins that appeared to bind stoichiometrically to Zds1 (Figure 2A). These proteins were identified by mass spectrometry as Cdc55, Tpd3, and Pph21/Pph22. The complex could be purified in the presence of 1 M KCl, which indicated a tight association.

The same protein complex also could be purified by using Zds1–3XHA expressed from its own promoter or by using Cdc55–3XHA expressed from its own promoter (data not shown). Tpd3 and Pph21/22 failed to copurify with Zds1 in *cdc55*Δ cells: This result indicated that Cdc55 mediates binding of Zds1 to PP2A (Figure 2A). Note that Zds1–3XHA showed a reduced electrophoretic mobility when isolated from *cdc55*Δ cells. This issue is addressed later in this article. Observation of *cdc55*Δ cells, in which Zds1/2 fail to interact with PP2A, revealed that they exhibit a morphological phenotype similar to the one observed in *zds1*Δ *zds2*Δ cells (Figure 2B). Together, these observations suggest that Zds1/2 mediate the functions of PP2A^{Cdc55} via binding to the Cdc55 subunit.

Zds1/2 target dephosphorylation of Mih1 by PP2A^{Cdc55}

We next sought to identify targets of the PP2A^{Cdc55}–Zds1/2 complex. Swe1 and Mih1 were good candidates because genetic analysis demonstrated that Zds1/2 regulate Cdk1 inhibitory phosphorylation (Figure 1; McMillan *et al.*, 1999). Moreover, previous work demonstrated that Mih1 and Swe1 undergo dramatic cell cycle–dependent changes in phosphorylation that may be regulated by PP2A^{Cdc55} (Sreenivasan and Kellogg, 1999; Harvey *et al.*, 2005; Pal *et al.*, 2008). We therefore used Western blotting to assay phosphorylation of Mih1 and Swe1 in synchronized *zds1*Δ *zds2*Δ cells that carry a mutant allele of *CDK1* that can not be inhibited by Swe1 (*cdk1-Y19F*). The *cdk1-Y19F* allele largely rescued the severe morphological defects and mitotic delay caused by *zds1*Δ *zds2*Δ, which allowed the cells to be synchronized (Figure S1). The *cdk1-Y19F* allele also removed the concern that effects of *zds1*Δ *zds2*Δ on regulation of Swe1 or Mih1 could be caused indirectly by inhibition of Cdk1, which is possible because Cdk1 regulates both Swe1 and Mih1 (Harvey *et al.*, 2005; Pal *et al.*, 2008). Thus, using *cdk1-Y19F* allowed us to focus on the role of Zds1/2 in signals that act upstream of Mih1 and Swe1. We assayed accumulation of the mitotic cyclin Clb2 in the same samples, which provided a molecular marker for mitotic progression (Figure 3C). Western blot signals in each strain were normalized to a loading control, so protein levels could be compared between strains.

In *cdk1-Y19F* control cells, Mih1 underwent dephosphorylation as cells entered mitosis, as previously observed in wild-type cells (Pal *et al.*, 2008) (Figure 3A). Strikingly, in *cdk1-Y19F zds1*Δ *zds2*Δ cells, Mih1 failed to undergo full dephosphorylation as cells entered mitosis. An identical effect was previously observed in *cdc55*Δ cells (Pal *et al.*, 2008).

The effects of *zds1*Δ *zds2*Δ on Swe1 phosphorylation were more subtle. In the *cdk1-Y19F* control cells, Swe1 initially accumulated in a partially hyperphosphorylated form (Figure 3B, band marked with one asterisk) and then accumulated in a fully hyperphosphorylated form (band marked with two asterisks), as previously reported in wild-type and *cdk1-Y19F* cells (Harvey *et al.*, 2005). In *cdk1-Y19F zds1*Δ *zds2*Δ cells, the Swe1 protein accumulated with timing that was similar to that of the control cells, but the initial phosphorylation of Swe1 was slightly delayed. In addition, a smaller amount of Swe1 reached full hyperphosphorylation, and Swe1 accumulated in the partially phosphorylated form (band marked with an asterisk in Figure 3B). These results were unexpected because, in independent experiments, we discovered that PP2A^{Cdc55} opposes phosphorylation of Swe1 by Cdk1/Clb2 (S. Harvey and D. Kellogg, unpublished data). Specifically, we found that the initial partial hyperphosphorylation of Swe1 occurred prematurely in *cdk1-Y19F cdc55*Δ cells. Diverse experiments suggest a model in which the opposing activity of PP2A^{Cdc55} creates a threshold that limits the initial activating phosphorylation of Swe1 by Cdk1, thereby allowing a low level of Cdk1 activity to escape Swe1 inhibition to initiate early mitotic events (S. Harvey and D. Kellogg, unpublished data). If Zds1/2 mediate the functions of PP2A^{Cdc55}, one would expect to see premature hyperphosphorylation of Swe1 in *cdk1-Y19F zds1*Δ *zds2*Δ cells.

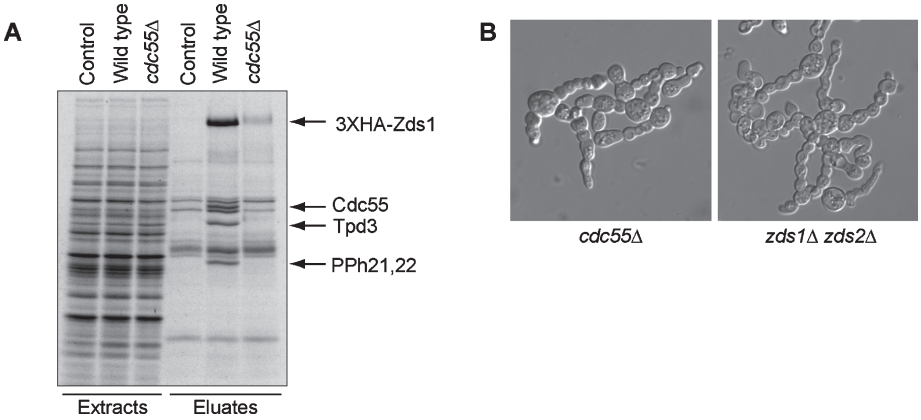

FIGURE 2: Zds1 interacts with PP2A^{Cdc55} via the Cdc55 subunit. (A) 3XHA-Zds1 complexes were purified from wild-type and *cdc55*Δ cells by immunoaffinity chromatography in the presence of 0.5M KCl using anti-HA antibodies. Columns were eluted with an excess of HA-dipeptide. Eluates were resolved by SDS–PAGE and stained with Coomassie blue. As a control, the same procedure was carried out in parallel by using a strain that did not carry HA-tagged Zds1 (lanes marked "Control"). Proteins identified by mass spectrometry are indicated at the right side of the gel. (B) Images of *cdc55*Δ and *zds1 zds2*Δ cells in logarithmic phase were taken after overnight growth in YPD at room temperature.

A model that could explain the different phenotypes caused by *cdc55*Δ and *zds1*Δ *zds2*Δ is that PP2A^{Cdc55} is active against Swe1 in the absence of Zds1/2 but strictly requires Zds1/2 for dephosphorylation of Mih1. To test this model, we deleted the *CDC55* gene in the *cdk1-Y19F zds1*Δ *zds2*Δ cells. This deletion caused premature phosphorylation of Swe1, loss of hypophosphorylated forms of Swe1, and accumulation of Swe1 in a partially phosphorylated form, as we observed in *cdk1-Y19F cdc55*Δ cells (Figure 1B) (S. Harvey and D. Kellogg, unpublished data). The failure of Mih1 to undergo dephosphorylation in *zds1*Δ *zds2*Δ cells was not affected by additional deletion of *CDC55*.

In summary, the data in Figure 3, A and B, demonstrate that Zds1/2 are strictly required for the PP2A^{Cdc55}-dependent dephosphorylation of Mih1, but are not required for the PP2A^{Cdc55}-dependent dephosphorylation of Swe1. Thus, Zds1/2 activate PP2A^{Cdc55}-dependent dephosphorylation of Mih1. In contrast, previous work reached the conclusion that Zds1/2 inhibit PP2A^{Cdc55}-dependent dephosphorylation of Net1, which suggests that they can play both positive and negative roles in the regulation of PP2A^{Cdc55} (Queralt and Uhlmann, 2008). This issue is addressed further in the *Discussion*.

Inactivation of Zds1/2 also caused subtle effects on the accumulation of Clb2 protein. Clb2 accumulation was delayed in *zds1*Δ *zds2*Δ *cdk1-Y19F* cells compared to *cdk1-Y19F* control cells (Figure 3C; peak Clb2 levels are marked with an asterisk), and overall levels of Clb2 appeared to be reduced. The delay in reaching peak levels was rescued by *cdc55*Δ. The causes of these effects are unknown. Several high-throughput screens identified physical interactions between Zds1/2 and proteins involved in transcription, so the effects on Clb2 accumulation could be due to a transcriptional role for Zds1/2. In addition, previous studies suggest that the effect of inactivating Zds1/2 on the timing of peak Clb2 levels may be due to a role for Zds1/2 in mitotic exit. In these studies, it was found that PP2A^{Cdc55} inhibits mitotic exit by opposing phosphorylation of Net1, which sequesters the Cdc14 phosphatase in the nucleolus (Queralt and Uhlmann, 2008). Phosphorylation of Net1 triggers release of Cdc14, which then promotes mitotic exit. Zds1/2 are thought to promote mitotic exit by inhibiting PP2A^{Cdc55}-dependent dephosphorylation of Net1 (Queralt and Uhlmann, 2008). Thus, PP2A^{Cdc55} should be hyperactive against Net1 in *zds1*Δ *zds2*Δ *cdk1-Y19F* cells. The hyperactivity should cause a delay in mitotic exit and a corresponding delay in destruction of Clb2 that should be eliminated by *cdc55*Δ, which is consistent with the observed effects of inactivating Zds1/2 on Clb2 levels (Figure 3C). Control of mitotic exit by PP2A^{Cdc55} is independent of Cdk1 inhibitory phosphorylation (Queralt *et al.*, 2006).

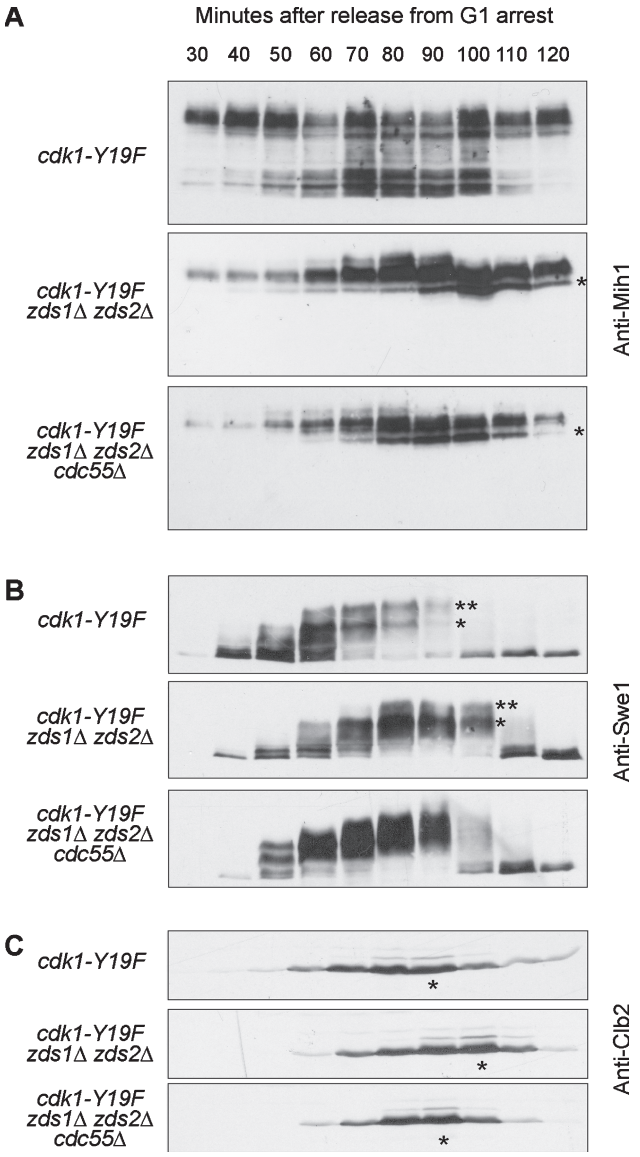

FIGURE 3: Zds1/2 target the activity of PP2A^{Cdc55} to Mih1. Wild-type, *zds1*Δ *zds2*Δ, and *zds1*Δ *zds2*Δ *cdc55*Δ cells in a *cdk1-Y19F* background were synchronized in G1 with α-factor at 25°C and released in fresh YPD at 30°C. Cells were harvested at the indicated time points, and extracts were analyzed by Western blotting using anti-Mih1 (A), anti-Swe1 (B), and anti-Clb2 (C) antibodies as indicated. Asterisks in (A) mark a slightly dephosphorylated form of Mih1. In (B), single asterisks mark a partially hyperphosphorylated form of Swe1, and double asterisks mark the fully hyperphosphorylated form. In (C), asterisks mark the peak levels of Clb2 before destruction was initiated. All samples in this figure are from the same experiment. A background band in another region of the gel was used to ensure that protein levels were normalized between strains. The data presented represent one of three completely independent experiments, all of which gave reproducible results.

The phosphorylation state of Zds1 is controlled by opposing kinase and phosphatase activities

The discovery that Zds1/2 bind tightly to PP2A^{Cdc55} and are required for dephosphorylation of Mih1 suggested that they may play a role in relaying upstream signals that control Mih1 during entry into mitosis. We therefore carried out experiments to identify mechanisms that could regulate Zds1. We noticed that Zds1 purified from *cdc55*Δ cells appeared to migrate with a slower electrophoretic mobility, which suggested hyperphosphorylation (Figure 2A). To confirm this, we used Western blotting to assay the electrophoretic mobility of Zds1 in crude extracts of wild-type and *cdc55*Δ cells. To improve resolution, electrophoresis was carried out for a longer period of time, which revealed a quantitative shift in Zds1 mobility in *cdc55*Δ cells (Figure 4A). Treatment of Zds1 isolated from *cdc55*Δ cells with phosphatase caused Zds1 to shift to a lower apparent molecular weight (Figure 4B). These observations demonstrate that Zds1 undergoes hyperphosphorylation when it is dissociated from PP2A^{Cdc55}. They also suggest that phosphorylation of Zds1 is normally opposed by PP2A^{Cdc55}. To further test this idea, we assayed Zds1 phosphorylation in cells that were dependent on a temperature-sensitive allele of one of the redundant PP2A catalytic subunits (*pph22–172 pph21*Δ *pph3*Δ) (Figure 4C) (Stark, 1996). This strain showed reduced growth

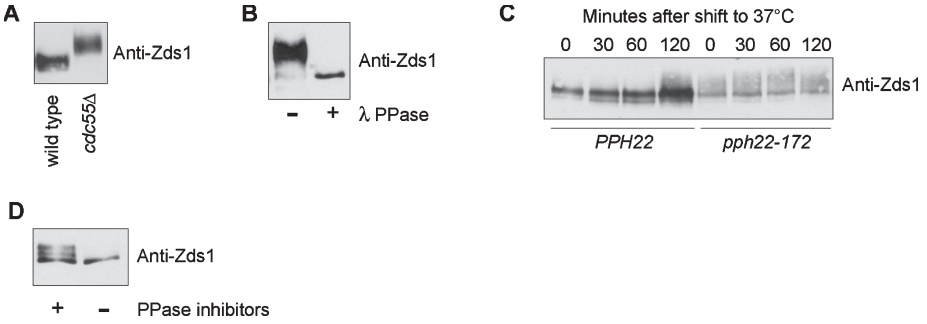

FIGURE 4: Zds1 undergoes phosphorylation and is regulated by PP2A^{Cdc55}. (A) Cell extracts of rapidly growing wild-type and *cdc55*Δ cells were analyzed by Western blotting using an anti-Zds1 antibody. (B) Zds1 was immunoprecipitated from *cdc55*Δ cells using anti-Zds1 antibodies bound to protein G beads. At the end of the purification, the beads were split in half and λ−phosphatase was added to one half. After a 30-min incubation at 30°C, the immunoprecipitates were boiled and analyzed by SDS–PAGE and Western blotting. (C) Asynchronous *pph21*Δ *pph3*Δ *pph22–172* and *pph21*Δ *pph3*Δ *PPH22* cells were shifted to the restrictive temperature (37°C) for the indicated times. Zds1 phosphorylation was analyzed by Western blotting. (D) Zds1 was immunoprecipitated from rapidly growing wild-type cells using anti-Zds1 antibodies bound to protein G beads in the presence or absence of phosphatase inhibitors. Immunoprecipitates were analyzed by SDS–PAGE and Western blotting.

at the permissive temperature, which indicated decreased PP2A function. We found that Zds1 was hyperphosphorylated at both the permissive and restrictive temperatures, which further confirmed that phosphorylation of Zds1 is opposed by PP2A^{Cdc55}. We showed that Zds1 is also phosphorylated in wild-type cells by immunoprecipitating Zds1 in the presence or absence of phosphatase inhibitors. In the absence of phosphatase inhibitors, Zds1 migrated more rapidly, which demonstrated that Zds1 became dephosphorylated during the immunoprecipitation, most likely by associated PP2A^{Cdc55} (Figure 4D).

Together, these results suggest that the phosphorylation state of Zds1 is determined by the opposing activities of PP2A^{Cdc55} and at least one kinase. Dissociation of Zds1 from PP2A^{Cdc55} shifts the balance entirely to the kinase, which causes Zds1 to undergo quantitative hyperphosphorylation.

Zds1 undergoes cell cycle–dependent phosphorylation

We next tested whether Zds1 undergoes cell cycle–dependent phosphorylation. To do this, we used Western blotting to follow the behavior of the Zds1 protein during the cell cycle in cells synchronized in G1 by centrifugal elutriation. To provide molecular markers for cell-cycle progression, we also monitored the behavior of the G1 cyclin Cln2 and the mitotic cyclin Clb2. Zds1 appeared as two bands in early G1 and shifted to a form with reduced electrophoretic mobility in late G1 phase (Figure 5A). The reduced mobility correlated with the appearance of Cln2. We observed the same result regardless of whether cells were synchronized by centrifugal elutriation (Figure 5A) or by α-factor arrest and release (Figure 5B).

We carried out a similar analysis in *zds1–1 zds2*Δ cells and *zds2*Δ control cells synchronized in G1 by mating pheromone arrest and release. This analysis revealed that the temperature-sensitive zds1–1 protein also showed reduced electrophoretic mobility that was strongly correlated with Cln2 levels (Figure 5B). The mobility shift was larger than that of the wild-type protein because the zds1–1 protein was hypophosphorylated in early G1 (Figure 5C). Treatment of the zds1–1 protein with phosphatase confirmed that it was full length, because it ran as a single band of the same molecular weight as that of dephosphorylated wild-type Zds1 (Figure 5D). The zds1–1 protein remained hyperphosphorylated after G1, in contrast to wild-type Zds1, which underwent partial dephosphorylation (Figure 5, A–C). Thus, zds1–1 is phosphorylated in late G1 similar to wild type but shows phosphorylation defects at other stages of the cell cycle, which may be the cause of the mutant phenotype.

These experiments also revealed that *zds1–1 zds2*Δ cells undergo a prolonged arrest with high levels of Cln2 and Clb2 at the restrictive temperature (Figure 5B). This finding supports a role for Zds1/2 in controlling activation of Cdk1/Clb2, because previous work demonstrated that Cdk1/Clb2 represses Cln2 transcription by phosphorylating the transcription factor that promotes G1 cyclin transcription (Amon *et al.*, 1993). Because Cdk1/Cln2 promotes polar growth, the failure to repress *CLN2* transcription is the likely cause of the elongated cell phenotype observed in the *zds1–1 zds2*Δ mutant.

Zds1 phosphorylation is partially dependent on Cdk1 associated with G1 cyclins

We next sought to identify the kinase or kinases responsible for Zds1 phosphorylation. Because the electrophoretic mobility shift of Zds1 and zds1–1 correlated with Cln2 levels, we asked whether Zds1 phosphorylation was dependent on Cdk1 activity. We used an analogue-sensitive allele of *CDK1* (*cdk1-as1*) that can be specifically and rapidly inhibited in vivo by the adenine analogue 1NM-PP1 (Bishop *et al.*, 2000). Inhibition of *cdk1-as1* in cells synchronized in G1 with peak Cln2 levels caused a fraction of Zds1 to undergo dephosphorylation within 2.5 min (Figure 6A). Treatment of wild-type cells with 1NM-PP1 did not cause a loss of Zds1 phosphorylation (data not shown). In contrast, inhibition of *cdk1-as1* in mitosis, when Cln2 was no longer present, had no effect on Zds1 phosphorylation, suggesting that Cdk1/Cln2, but not Cdk1/Clb2, is required for full phosphorylation of Zds1. In agreement with these observations, we found that Zds1 was significantly less phosphorylated in *cln1*Δ *cln2*Δ cells and that overexpression of Cln2 led to a slight increase in Zds1 phosphorylation (Figure 6B).

To examine whether Zds1 is a direct substrate of Cln2/Cdk1, we performed an in vitro kinase assay. We purified Cdk1/Cln2–3XHA, Cdk1/Clb2–3XHA and 3XHA-Zds1 by immunoaffinity chromatography with specific peptide elution. The 3XHA-Zds1 was purified from *cdc55*Δ cells to remove associated PP2A^{Cdc55} and was treated with phosphatase prior to elution to eliminate Zds1 phosphorylation. Incubation of Zds1 with Cdk1/Cln2 resulted in hyperphosphorylation of Zds1, whereas Cdk1/Clb2 was unable to phosphorylate Zds1, even though Cdk1/Clb2 was present in excess in comparison to Cdk1/Cln2 (Figure 6C, right panel). Thus, Cdk1/Cln2 shows strong specificity in phosphorylation of Zds1, which supports the idea that Cdk1/Cln2 phosphorylates Zds1 in vivo.

Two observations suggest that kinases other than Cdk1/Cln2 must contribute to phosphorylation of Zds1 in vivo. First, Zds1 did not undergo full dephosphorylation after inhibition of cdk1-as1 (Figure 6A) or in *cln1*Δ *cln2*Δ cells (Figure 6B). Second, the disappearance of Cln2 prior to entry into mitosis did not lead to a complete dephosphorylation of Zds1 (Figure 5, A and B). Thus, it appears that Zds1 is regulated by multiple kinases.

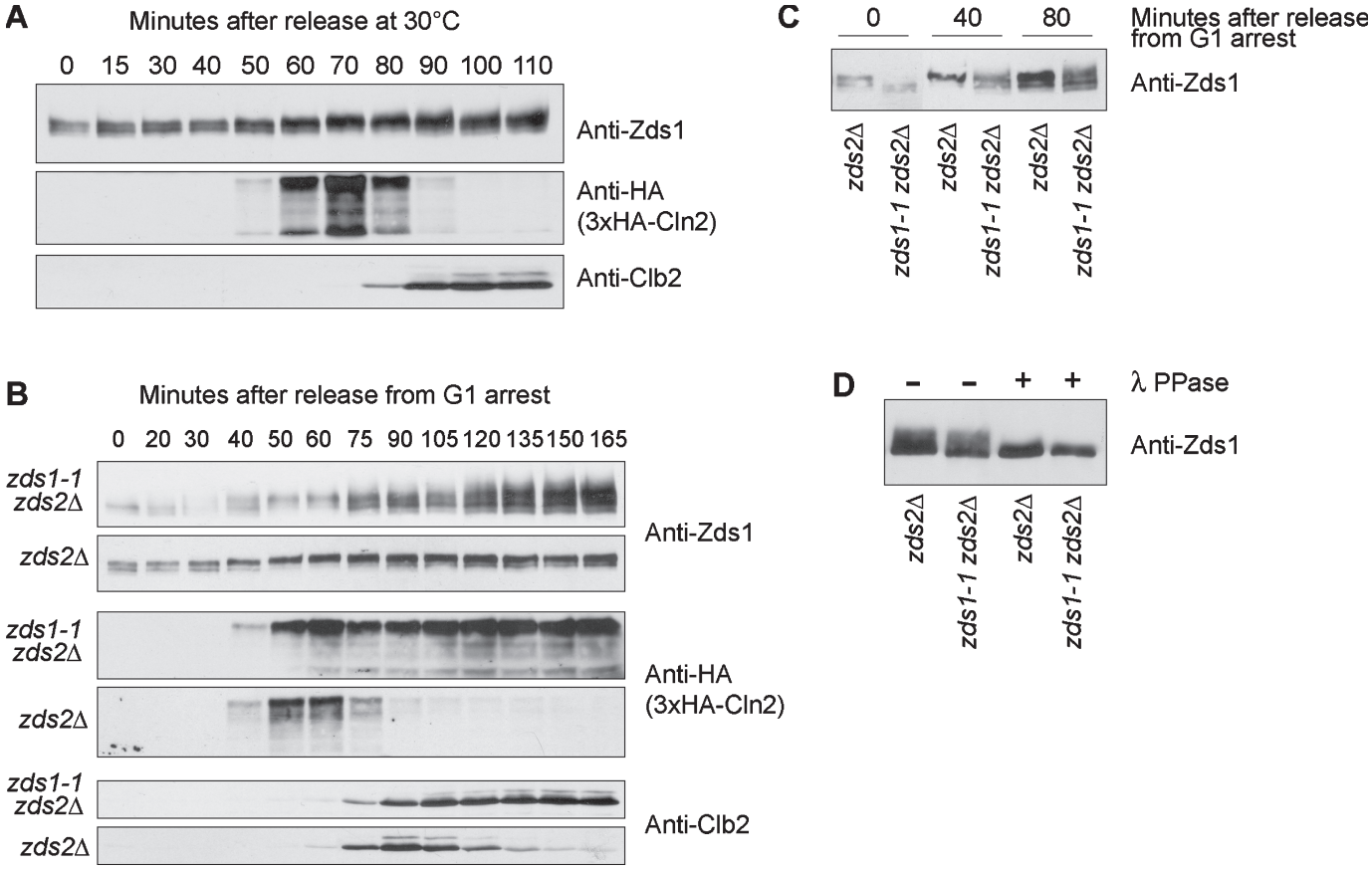

FIGURE 5: Zds1 undergoes cell cycle–dependent phosphorylation. (A) Small unbudded wild-type cells that express 3XHA-tagged Cln2 were isolated by centrifugal elutriation. Cells were released into fresh YPD at 30°C, and samples were taken at the indicated time points. Each sample was analyzed by Western blotting using anti-Zds1, anti-HA, and anti-Clb2 antibodies. (B) *zds2*Δ and *zds1–1 zds2*Δ cells that express 3XHA-tagged Cln2 were arrested in G1 with α-factor at 25°C and released into fresh YPD at 34°C. Samples were taken at the indicated time points and analyzed by Western blotting using anti-Zds1, anti-HA, and anti-Clb2 antibodies. (C) Side-by-side comparison is shown of the electrophoretic mobility of Zds1 and zds1–1 by Western blotting at the indicated time points after α-factor arrest and release. (D) Zds1 and zds1–1 were immunoprecipitated from *zds2*Δ and *zds2*Δ *zds1–1* cells, respectively, using anti-Zds1 antibodies bound to protein G beads. At the end of the purification, the beads of each purification were split in half and λ–phosphatase was added to one half. After a 30-min incubation at 30°C, immunoprecipitates were boiled and analyzed by SDS–PAGE and Western blotting.

DISCUSSION

Inhibitory phosphorylation of Cdk1 controls entry into mitosis in all eukaryotic cells, yet the signals that control addition and removal of inhibitory phosphorylation are poorly understood. Previous work found that Zds1/2 are required for normal control of Cdk1 inhibitory phosphorylation; however, it was unclear whether they work in signaling mechanisms that directly control Cdk1 inhibitory phosphorylation or whether their inactivation affects Cdk1 phosphorylation indirectly by causing a failure in an early cell cycle event that triggers a checkpoint response. We therefore examined the functions of Zds1/2 to more clearly define their role in entry into mitosis.

We discovered that Zds1 forms a tight stoichiometric complex with $PP2A^{Cdc55}$ via an association with the Cdc55 subunit. This discovery complements and extends previous work that detected an association between Zds1/2 and $PP2A^{Cdc55}$ in coimmunoprecipitation assays, and it suggests that the primary role of Zds1/2 is to mediate the function or regulation of $PP2A^{Cdc55}$ (Gavin *et al.*, 2002; Collins *et al.*, 2007; Queralt and Uhlmann, 2008; Yasutis *et al.*, 2010). Because $PP2A^{Cdc55}$ acts directly on Mih1, Zds1/2 is placed immediately upstream of Mih1 (Pal *et al.*, 2008). Surprisingly, we found that Zds1/2 are required for $PP2A^{Cdc55}$-dependent dephosphorylation of Mih1 but not for $PP2A^{Cdc55}$-dependent dephosphorylation of Swe1, which demonstrates that they target $PP2A^{Cdc55}$ to Mih1. Zds1 undergoes complex cell cycle–dependent changes in phosphorylation, which suggests that Zds1/2 may be targets of upstream signals that control entry into mitosis. Together, these observations suggest a model in which Zds1/2 control Cdk1 inhibitory phosphorylation by relaying upstream signals that control entry into mitosis to Mih1 via $PP2A^{Cdc55}$. In this model, inactivation of Zds1/2 causes a mitotic arrest because the signal to remove Cdk1 inhibitory phosphorylation is not properly relayed. Although we favor this model, we cannot rule out the possibility that inactivation of Zds1/2 triggers a checkpoint arrest by causing defects in early cell-cycle events that could not be detected by our assays. It is also possible that Zds1/2 regulate entry into mitosis via additional mechanisms that are independent of $PP2A^{Cdc55}$ and Mih1.

Our understanding of the function of Zds1/2 is currently limited because we do not yet have comprehensive data on the functional consequences of dephosphorylation of Mih1 by $PP2A^{Cdc55}$-Zds1/2. To rigorously determine the functional significance of Mih1 dephosphorylation it will be necessary to assay the activity of differently phosphorylated forms of Mih1 and to map and mutate the relevant

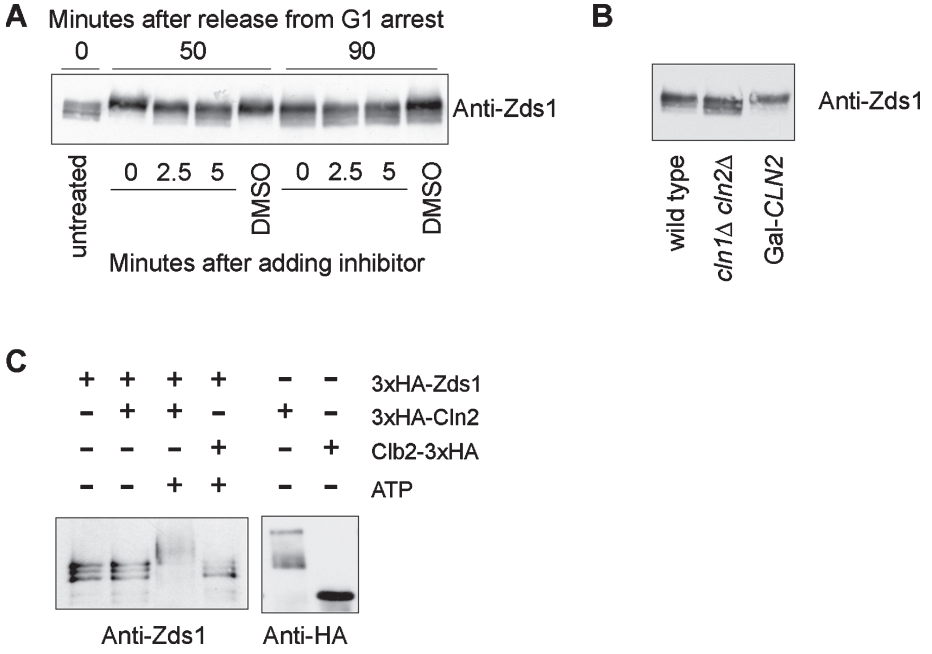

FIGURE 6: Cdk1 associated with G1 cyclins phosphorylates Zds1. (A) *cdk1-as1* cells were arrested with α-factor and released into fresh YPD at 30°C. 1NM-PP1 was added at 50 min (late G1) or 90 min (mitosis) after release, and samples were taken at the indicated times and analyzed by Western blotting to detect Zds1. As a control, DMSO was added to parallel samples for 5 min. (B) Wild-type cells, *cln1*Δ *cln2*Δ cells, and wild-type cells that overexpress Cln2 were grown to logarithmic phase either in YPD media (wild type, *cln1*Δ *cln2*Δ) or in synthetic defined URA media containing 2% galactose (*GAL1-CLN2*), and the behavior of Zds1 was analyzed by Western blotting. (C) Purified 3XHA-Zds1 (10 μl) was incubated with 10 μl of the indicated purified proteins in the presence or absence of ATP at 30°C for 30 min, and the behavior of Zds1 was monitored by Western blotting. In the second panel, equal amounts of purified 3XHA-Cln2/Cdk1 or Clb2-3XHA/Cdk1 were loaded on a separate gel and analyzed by Western blotting using anti-HA antibodies to allow comparison of protein levels of the purified Cdk1 complexes.

phosphorylation sites, which has not yet been possible. Several observations suggest, however, that Yck1/2-dependent phosphorylation inhibits Mih1 activity and that dephosphorylation leads to increased Mih1 activity. First, Yck1/2-dependent hyperphosphorylation of Mih1 occurs during interphase, when Mih1 activity should be suppressed, and $PP2A^{Cdc55}$-Zds1/2 dephosphorylates Mih1 during entry into mitosis, when Mih1 activity must be increased (Pal *et al.*, 2008). Second, *cdc55*Δ causes a failure in Mih1 dephosphorylation, increased Cdk1 inhibitory phosphorylation, and severe defects in entry into mitosis that are rescued by *swe1*Δ (Minshull *et al.*, 1996; Yang *et al.*, 2000; Pal *et al.*, 2008). Finally, *zds1*Δ *zds2*Δ causes a complete failure in Mih1 dephosphorylation and severe defects in entry into mitosis, even though $PP2A^{Cdc55}$ retains activity against Swe1. The facts that Zds1/2 play a specific role in targeting $PP2A^{Cdc55}$ to Mih1 and that loss of Zds1/2 causes severe defects in entry into mitosis strengthen the evidence that removal of Yck1/2-dependent Mih1 phosphorylation promotes entry into mitosis. Inactivation of Yck1/2 causes a failure in Mih1 hyperphosphorylation but does not cause premature entry into mitosis, as would be predicted if Yck1/2 inhibited Mih1 (Pal *et al.*, 2008). Preliminary experiments suggest, however, that Yck1/2 may also be required for inactivation of Swe1, which complicates interpretation of the phenotype caused by loss of Yck1/2 (S. Anastasia and D. Kellogg, unpublished data).

The hyperphosphorylation of Mih1 early in interphase contrasts with Xenopus Cdc25, which is not hyperphosphorylated during interphase. A possible explanation is that hyperphosphorylation of Mih1 early in the cell cycle reflects an added layer of checkpoint control that does not operate in Xenopus egg extracts. In budding yeast, Wee1 and Cdc25 respond to checkpoint signals that coordinate entry into mitosis with bud growth or morphogenesis, whereas in early Xenopus embryos, cell division occurs without accompanying growth or morphogenesis. Hyperphosphorylation of Mih1 early in the cell cycle may therefore inhibit Mih1 until bud growth or morphogenesis is complete. In this model, Zds1/2 would play a critical role in relaying checkpoint signals that trigger dephosphorylation of Mih1 when checkpoint conditions have been satisfied. Interestingly, inhibition of PP2A in interphase Xenopus extracts leads to extensive and quantitative hyperphosphorylation of Cdc25 in the absence of mitotic Cdk1 activity (Kumagai and Dunphy, 1992; Izumi and Maller, 1995). Although the identity of the kinase is unknown, this observation suggests that the potential for similar checkpoint signaling may exist in vertebrate cells and that the checkpoint is turned off in Xenopus oocytes.

Previous work reached the conclusion that Zds1/2 inhibit the activity of $PP2A^{Cdc55}$ against Net1 (Queralt and Uhlmann, 2008). Interestingly, the behavior of Swe1 in cells that lack Zds1/2 is also consistent with an inhibitory role for Zds1/2. In this case, the delayed phosphorylation of Swe1 and accumulation of Swe1 in an intermediate phosphorylation form could be explained by a role for Zds1/2 in inhibiting the activity of $PP2A^{Cdc55}$ against Swe1. Because $PP2A^{Cdc55}$ opposes phosphorylation of Swe1 by Cdk1/Clb2, hyperactivity of $PP2A^{Cdc55}$ in the absence of Zds1/2 would lead to decreased phosphorylation of Swe1, which is consistent with the observed behavior of Swe1 in *zds1*Δ *zds2*Δ *cdk1-Y19F* cells. These observations suggest the possibility that Zds1/2 are capable of playing both activating and inhibitory roles in the regulation of $PP2A^{Cdc55}$. Cell cycle–dependent changes in phosphorylation of Zds1/2 could determine whether they play activating or inhibitory roles. An interesting possibility is that a change in the phosphorylation state of Zds1/2 during entry into mitosis leads to inhibition of $PP2A^{Cdc55}$ activity against Swe1 and to stimulation of $PP2A^{Cdc55}$ activity against Mih1. This would simultaneously promote full hyperphosphorylation and inactivation of Swe1, as well as dephosphorylation and activation of Mih1. In this model, mechanisms that regulate $PP2A^{Cdc55}$ could promote mitotic progression via coordinated inhibition of Swe1 and activation of Mih1. This could be achieved in a relatively simple manner. For example, a change in Zds1/2 phosphorylation could target $PP2A^{Cdc55}$ to Mih1, thereby pulling active $PP2A^{Cdc55}$ away from Swe1.

An intriguing finding was that Zds1 becomes quantitatively hyperphosphorylated when it is dissociated from the $PP2A^{Cdc55}$ complex. This finding suggests that Zds1 is continuously being dephosphorylated by associated $PP2A^{Cdc55}$ and that its phosphorylation state is determined in a highly dynamic manner by opposing kinase and phosphatase activities. Theoretical considerations have shown that a kinase and phosphatase acting on the same target protein can generate switchlike behavior (Goldbeter and Koshland, 1981,

1984; Ferrell, 1996). If the kinase and phosphatase operate at or near their maximal velocities, the target protein can exhibit large switchlike changes in its phosphorylation state in response to small changes in enzyme velocity. This behavior is referred to as "zero-order ultrasensitivity." The fact that $PP2A^{Cdc55}$ is associated with Zds1/2 suggests that it is acting at its maximal velocity, which fulfills one requirement for a zero-order ultrasensitivity. Thus the $PP2A^{Cdc55}$-Zds1/2 complex may contribute to switchlike activation of Cdk1 during entry into mitosis.

The discovery that Zds1 undergoes cell cycle–dependent changes in phosphorylation raises the possibility that regulation of $PP2A^{Cdc55}$ plays an important role in the mechanisms that trigger entry into mitosis. An interesting model is that phosphorylation of Zds1/2 by Cdk1/Cln2 early in the cell cycle inhibits their ability to target dephosphorylation of Mih1. Because Cdk1/Cln2 drives bud growth, this would ensure that entry into mitosis does not occur while bud growth is ongoing (McCusker *et al.*, 2007). The fact that multiple signals feed into Zds1/2 suggests that they could be an integration point for checkpoint signals that report on the status of cell size or morphogenesis. Zds1 is localized to the growing bud, so it is well positioned to relay these kinds of signals (Bi and Pringle, 1996). An important goal for future work will be to fully define the signals that control Zds1/2, as this will likely lead to a better understanding of the checkpoint signals that control entry into mitosis.

MATERIALS AND METHODS

Yeast strains and culture conditions

The strains used in this study are listed in Table 1. All yeast strains are in the W303 background (*his3–11,15, leu2–3,112, trp1–1, ura3–52, ade2–1, can1–100*) except YDH6 and YDH8, which are in the YPH250 background (*trp1-Δ1 his3-Δ200 leu2-Δ1 lys2–801*^{amber} *ade2–101 ura3–52*) and DK608, which was created by sporulating a ZDS2/zds2Δ::KanMX diploid from the BY4743 background (*his3Δ1/his3Δ1, leu2Δ0/leu2Δ0, LYS2/lys2Δ0, met15Δ0/MET15, ura3Δ0/ura3Δ0*). Unless otherwise indicated, all strains were grown in yeast extract–peptone–dextrose (YPD) medium supplemented with 40 mg/l adenine. Experiments using the *cdk1-as1* strain (JAU05) were carried out in YPD lacking supplemental adenine. DK589 was generated by transformation of DK186 with the *pGAL-CLN2* plasmid (a gift of Ray Deshaies, California Institute of Technology, Pasadena, CA). DK599 was generated by sporulation of a diploid generated by crossing HT138 with ADR473. HT125, HT126, HT127, and HT128 were generated by sporulating the diploid DY4036. HT133 was generated by sporulating the diploid DY4037. HT138 was generated by integrating a PCR product containing the *GAL1* promoter and a 3XHA tag upstream of *ZDS1* in strain DK186 (Longtine *et al.*, 1998). HT153 and HT216 were obtained by sporulation of diploids generated by crossing HT133 with RA5 and HT126 with AS1, respectively. SW49 was obtained from a cross between HT126 and ADR489. DK608 was obtained by sporulation of a *zds2::kanMX4/ZDS2* strain obtained from Open Biosystems Products (Huntsville, AL). SW61 and SW62 were obtained by sporulation of SW52, which was obtained by crossing SW49 with DK608. SW117 was generated by sporulation of a diploid obtained by crossing HT125 with SW116. SW116 was created by crossing HT128 and ADR510. To generate SW129, *CDC55* was deleted in SW117 using a PCR-based approach (oligos: GGAGAGATCTTACGCATAAA-GAAATATAATATAGCGCA-CACGGATCCCCGGGTTAATTAA and CAGTAGTAGTATGT-GGG-GAAGATATGGGATAAAAAAAAGTGAATTCGAGCTCGTTTAAAC, vector: pFA6a-kanMX6) (Longtine *et al.*, 1998). SW77, SW80, SW127, and SW131 were obtained by integrating pDK31B (CLN2–3XHA, ADE2, LEU2) into SW34, SW24, ADR510, and SW117 at the CLN2 locus.

Generation of ZDS1 temperature-sensitive alleles

To generate *zds1-ts* alleles, the *Schizosaccharomyces pombe his5*$^{+}$ gene was integrated downstream of *ZDS1* in strain HT127 using a standard PCR-based approach to create strain SW24 (oligos: GGGAAAGTTGGACAAACACCAAACTTCTCATAATACAATCG-GATCCCCGGGTTAATTAA and GGCACATTTTCTTCCGGCCG-CAGAAAGCTCTCTTTATCAGAATTCGAGCTCGTTTAAAC; vector: pFA6a-His3MX6) (Longtine *et al.*, 1998). The *ZDS1* gene and the downstream *his5*$^{+}$ gene were then amplified under mutagenic conditions (oligos: CACCACCAGGGTGTTCGCTC and CGCACT-GCTGGTCCTTGG), and the PCR product was transformed into HT127. Colonies were screened at the restrictive temperature for slow growth and rough colony morphology, which are characteristic of a loss of *ZDS1/2* function. As a secondary screen, cells were examined to determine whether they have elongated buds at 37°C, which is a further indication of a loss of *ZDS1/2* function. All of the *zds1-ts* mutants could be rescued by a CEN plasmid that carries wild-type *ZDS1* (pSM1), which was constructed by cloning *ZDS1* into Ycplac33 (oligos: CGCGGATCCCTCTGGTAGGAACTC-CTGGTT and CGCGCTGCAGTTGATAAGTGACCC-AGCAGTC).

Antibody generation, Western blotting, and microscopy

To generate an anti-Zds1 antibody, the Zds1 sequence encoding amino-acid residues 183 through 393 was cloned into pGEX4T-3 to create pHT52 (oligos: CGCGGATCCGCG-GGTGAAGATAATGAT-GGG and CCGGAATTCCGGGTCGTCGTTTTTCATTTCATCCAC). The GST-Zds1(183–393) fusion was expressed in *Escherichia coli* and purified as previously described (Kellogg and Alberts, 1992). SDS–PAGE was performed as previously described (Anderson *et al.*, 1973). Gel electrophoresis for analysis of Zds1 phosphorylation by Western blotting was performed with a 9% SDS–PAGE gel of dimensions 17 cm × 8.5 cm × 1 mm. The gels were run at 20 mA on the constant current setting until a 97-kD prestained molecular mass marker was near the bottom of the gel. Western blot transfers were performed for 1 h at 1 A at 4°C in a Hoefer (Holliston, MA) transfer tank in a buffer containing 20 mM Tris base, 150 mM glycine, and 20% methanol. Gel electrophoresis for analysis of Swe1 and Mih1 phosphorylation by Western blotting was performed as previously described (Harvey *et al.*, 2005; Pal *et al.*, 2008). For immunofluorescence assays, cells were fixed and stained with anti-tubulin or anti-Cdc11 antibodies, as previously described (Pringle *et al.*, 1991). Fluorescence pictures were taken using a Nikon Eclipse TS100 and a Nikon ELWD 0.3 camera with a 100× 1.4 aperture objective. Differential interference contrast images were taken using a Zeiss Axioskop 2 (Carl Zeiss) and an AxioCam HRm camera with a 100× 1.3 numerical aperture objective.

Cell-cycle time courses, centrifugal elutriation, and other time courses

For cell-cycle time courses, log-phase culture cells were grown overnight to optical density $(OD)_{600}$ = 0.7 at room temperature. Cells were arrested in G1 by addition of α-factor at 15 μg/ml for 2.5 h at 25°C. The cells were released from the arrest by washing into prewarmed medium at 30°C, except for SW24, SW34, SW77, and SW80, which were released at 34°C. Samples (1.6 ml) were collected at 10-min intervals, and cells were rapidly pelleted and frozen in liquid nitrogen. Lysates were prepared by bead beating in the presence of 250 μl of acid-washed beads and 100 μl of protein sample buffer (65 mM Tris-HCl, pH 6.8, 3% SDS, 10% glycerol, 5%

Strain	Genotype	Reference or source
ADR473	*MATα, cdc55::LEU2*	Adam Rudner
ADR489	*MATa, cdc55::HIS3*	Adam Rudner
ADR510	*MATa, cdk1-Y19F-HA::URA3*	Adam Rudner
AS1	*MATa, bar1Δ elm1::TRP1*	Sreenivasan and Kellogg (1999)
DK177	*MATa*	Altman and Kellogg (1997)
DK186	*MATa, bar1Δ*	Altman and Kellogg (1997)
DK303	*MATa, bar1Δ CLB2–3XHA::TRP1*	Harvey *et al.* (2005)
DK589	*MATa, bar1Δ (pGAL-CLN2(CEN/URA3))*	This study
DK599	*MATa, bar1Δ cdc55::LEU2 GAL1–3XHA-ZDS1::his5$^+$ (S. pombe)*	This study
DK608	*MATα, zds2::kanMX6*	This study
DEY213	*MATa, bar1Δ PPH22::URA3 pph3Δ1::LYS2 pph21Δ::HIS3*	Evans and Stark (1997)
DEY214	*MATa, bar1Δ pph22–12::URA3 pph3Δ1::LYS2 pph21Δ::HIS3*	Evans and Stark (1997)
DMY305	*MATa, bar1Δ GAL1–3XHA-CLN2::TRP1*	McCusker *et al.* (2007)
DY4036	*MAT a/α, zds1::LEU2/ZDS1 zds2::TRP1/ZDS2*	David Stillman
DY4037	*MAT a/α, zds1::URA3/ZDS1 zds2::HIS3/ZDS2*	David Stillman
JAU05	*MATa, bar1Δ cdk1::cdk1-as1*	Bishop et al. (2000)
HT125	*MATa, zds1::LEU2*	This study
HT126	*MATα, zds1::LEU2*	This study
HT127	*MATa, zds2::TRP1*	This study
HT128	*MATα, zds2::TRP1*	This study
HT133	*MATa, zds1::URA3*	This study
HT138	*MATa, bar1Δ GAL1–3XHA-ZDS1:: his5$^+$ (S. pombe)*	This study
HT153	*MATα, ZDS1::URA3 gin4::LEU2*	This study
HT216	*MATa, ZDS1::LEU2 elm1::TRP1*	This study
KA61	*MATa, bar1Δ cln1Δ::TRP1 cln2Δ::LEU2*	Egelhofer et al. (2008)
RA5	*MATα, bar1Δ gin4::LEU2*	Altman and Kellogg (1997)
RA19	*MATa, bar1Δ gin4::LEU2*	Egelhofer *et al.* (2008)
SW24	*MATa, zds2::TRP1 ZDS1:: his5$^+$ (S. pombe)*	This study
SW34	*MATa, zds2::TRP1 zds1–1:: his5$^+$ (S. pombe)*	This study
SW49	*MATa, zds1::LEU2 cdc55::HIS3*	This study
SW52	*MATa/α, ZDS1/zds1::LEU2 ZDS2/zds2::kanMX6 CDC55/cdc55::HIS3*	This study
SW61	*MATα, cdc55::HIS3*	This study
SW62	*MATα, zds1::LEU2 zds2::kanMX6*	This study
SW77	*MATa, zds2::TRP1 zds1–1:: his5$^+$ (S. pombe) CLN2–3XHA::ADE2*	This study
SW80	*MATa, zds2::TRP1 ZDS1:: his5$^+$ (S. pombe) CLN2–3XHA::ADE2*	This study
SW116	*MATα zds2::TRP1 cdc28-Y19F-HA::URA3*	This study
SW117	*MATa, zds1::LEU2 zds2::TRP1 cdc28-Y19F-HA::URA3*	This study
SW127	*MATa, cdk1-Y19F-HA::URA3 CLN2–3XHA::ADE2*	This study
SW129	*MATa, zds1::LEU2 zds2::TRP1 cdc55::kanMX6 cdk1-Y19F-HA::URA3*	This study
SW131	*MATa, zds1::LEU2 zds2::TRP1 cdk1-Y19F-HA::URA3 CLN2–3XHA::ADE2*	This study

TABLE 1: Strains used in this study.

beta-mercaptoethanol) supplemented with 50 mM NaF, 50 mM beta-glycerophosphate, and 2 mM phenylmethylsulfonyl fluoride (PMSF). Bead beating was carried out with a Multibeater-8 (BioSpec Products, Bartlesville, OK) at top speed for 100 s. Lysates were incubated in a boiling water bath for 5 min and centrifuged for 5 min in a tabletop microfuge at top speed. Then, 20 μl was loaded on a gel. For Figure 1, D–F, 1-ml samples were collected for each time point and immediately fixed with 4% formaldehyde. At the end of the time course, cells were washed in 1X phosphate-buffered saline (PBS) and either analyzed directly under the microscope for bud emergence (Figure 1E) or processed for immunofluorescence (Figure 1, D and F). For Figure 6A, cells were released from α-factor arrest into fresh YPD at 30°C and split into four tubes. At 50 min, 25 μM 1NM-PP1 (a gift from C. Zang and K. Shokat, University of California, San Francisco) was added to one tube, and an equivalent amount of dimethyl sulfoxide (DMSO) was added to a second tube. Samples (1 ml) were collected at 0, 2.5, and 5 min (1NM-PP1) or at 5 min (DMSO) after treatment. The same procedure was used with the two remaining tubes at 90 min after release from α-factor arrest. For Figure 5A, small, unbudded cells were isolated by centrifugal elutriation from logarithmically growing cells in a Beckman Coulter J6-MI centrifuge and a JE-5.0 rotor at 4°C as previously described (Schwob and Nasmyth, 1993). The time-course experiment was carried out at 30°C, collecting 1-ml samples at the indicated time points. To test whether PP2A acts on Zds1, log-phase cultures of temperature-sensitive alleles of *PPH22* were shifted to the restrictive temperature (37°C), and 1.6-ml samples were collected at the indicated time points (Figure 4C).

Immunoaffinity purifications and mass spectrometry

Immunoaffinity purifications of 3XHA-Zds1 complexes (Figure 3A) were carried out in the presence of 0.5 M KCl using the same protocol as that used for purification oh 3XHA-Mih1, with some modifications (Pal *et al.*, 2008). Cells containing a 3XHA-Zds1 under the

control of the *GAL1* promoter (HT138, DK599) and control cells (DK186) were grown overnight at 30°C in yeast extract peptone medium containing 2% glycerol and 2% ethanol to OD_{600} = 0.8. Galactose was then added to 2% and the cells were incubated for 3 h at 30°C to induce 3XHA-Zds1 synthesis. Preparation of cell extracts, immunoaffinity beads, and incubation of extract with the anti–HA antibody beads was carried out exactly as described, except that the extract buffer contained 0.5 M KCl rather than 1 M KCl (Pal *et al.*, 2008). At the end of the incubation, the beads were washed two times with 15 ml of ice-cold extract buffer without PMSF. The beads were then transferred to a 1.5-ml Biospin column (Bio-Rad, Hercules, CA) and washed five times with 1 ml of extract buffer without PMSF and two times with 1 ml of extract buffer without PMSF or Tween 20. To elute the column, 250 μl of elution buffer containing HA dipeptide at 0.5 μg/ml was added to the column. After a 30-min incubation at room temperature, another aliquot was added and the flow-through fraction was collected. This process was repeated for a total of four fractions. The fractions were combined and flash frozen in liquid nitrogen. For mass spectrometry, 600 μl of eluate was precipitated in the presence of 10% trichloroacetic acid for 10 min on ice, followed by centrifugation for 5 min in a tabletop microfuge at 13,000 rpm. The pellet was resuspended in 50 μl of protein sample buffer, boiled for 5 min, and centrifuged for 5 min, then 25 μl was loaded on a 9% SDS-polyacrylamide gel. Protein bands were stained with Coomassie blue, then were excised and analyzed by mass spectrometry. Gel bands were digested with trypsin as previously described (Wilm *et al.*, 1996), and proteins were identified with a nano-LC ion source coupled to a Finnigan LCQ tandem mass spectrometer (Gatlin *et al.*, 1998). The tandem mass spectra were searched against the yeast open reading frame database obtained from Stanford University using the SEQUEST algorithm (Eng *et al.*, 1994). Each tandem mass spectrum that had a high scoring match was manually inspected to ensure that the match was correct.

The protocol used to purify 3XHA-Cln2/Cdk1 for kinase assays was the same as the one used for 3XHA-Zds1, with the following modifications: Cell expressing 3XHA-Cln2 under the control of the *GAL1* promoter (DMY305) were grown at 30°C to OD_{600} = 0.8 and induced as described earlier in text for 3XHA-Zds1. Cells (10 g) and 20 ml of extract buffer were used to prepare the extract. The extract buffer used was the same as the one used for 3XHA-Zds1 purification, except that it also contained 100 mM beta-glycerophosphate, 50 mM NaF, 1 mM vanadate, and 1 mM dithiothreitol (DTT). The elution buffer was the same as the one used for 3XHA-Zds1 elution. To purify Clb2–3XHA/Cdk1, 1.5 l of cells (DK303) was grown in YPD at 30°C to OD_{600} = 0.8. Cells were pelleted and resuspended in 1.6 l of YPD containing benomyl at 20 mg/l. After a 3-h incubation at room temperature, cells were washed with 50 mM HEPES-KOH, pH 7.6, and frozen in liquid nitrogen. Cells (6 g) and 13 ml of extract buffer were used to prepare the extract. The same protocol used to purify 3XHA-Zds1 was then followed. The purification of dephosphorylated 3XHA-Zds1 was carried out as described earlier in the text for 3XHA-Zds1 with the following modifications: At the end of the 3-h incubation, the beads were washed two times with 15 ml of extract buffer and once with 15 ml of lambda-phosphatase buffer (New England Biolabs, Ipswich, MA; 50 mM HEPES-KOH, pH 7.5, 100 mM NaCl, 2 mM DTT, 0.01% Brij 35, 1 mM $MnCl_2$). The beads were transferred to a 1.5-ml conical tube, and the supernatant was aspirated. Phosphatase buffer (100 μl) and 20 μl of lambda-phosphatase (New England Biolabs; 400,000 U/ml) were added. The beads were incubated for 2 h at 30°C. Phosphatase buffer (100 μl) was added, and the 1.5-ml tube containing the beads was placed on a rotator and incubated overnight at 4°C. The beads were transferred into a 15-ml conical tube, washed two times with extract buffer, transferred onto a 1.5-ml Bio-Spin column (Bio-Rad), and washed and eluted as described earlier in the text for 3XHA-Zds1.

In vitro kinase assays

In vitro kinase assays using purified dephosphorylated 3XHA-Zds1, 3XHA-Cln2/Cdk1, and Clb2–3XHA/Cdk1 were carried out as follows: 25-μl reactions containing 10 μl of eluate of dephosphorylated 3XHA-Zds1 and 10 μl of eluate of either 3XHA-Cln2-Cdk1 or Clb2–3XHA-Cdk1 were prepared in kinase assay buffer (50 mM HEPES-KOH, pH 7.6, 2 mM $MgCl_2$, 0.05% Tween-20, 10% glycerol, 1 mM DTT, all final concentrations) in the presence or absence of 1 mM ATP. Reactions were incubated at 30°C for 30 min and were terminated by freezing in liquid nitrogen. Then, 4 μl of 4X protein sample buffer was added, and samples were incubated in a boiling water bath for 3 min and resolved on a 9% SDS-polyacrylamide gel. To assess relative levels of each cyclin, 2 μl of 3XHA-Cln2/Cdk1 eluate and 2 μl of Clb2–3XHA/Cdk1 eluate were diluted in sample buffer and loaded onto a 10% SDS-polyacrylamide gel. Gels were analyzed by Western blotting using anti-Zds1 and anti-HA antibodies. The activity of Clb2–3XHA/Cdk1 was confirmed by performing the in vitro kinase assay with dephosphorylated Mih1 as substrate instead of Zds1 (see Pal *et al.*, 2008).

ACKNOWLEDGMENTS

S.W. was supported by a fellowship from the Swiss National Foundation. This work was supported by the Pew Biomedical Scholars Program and by Grant GM069062 from the National Institutes of Health. We thank members of the Kellogg lab for helpful discussions and critical reading of the manuscript, and we thank Michael Polymenis for supporting S.W. during this work.

REFERENCES

Altman R, Kellogg DR (1997). Control of mitotic events by Nap1 and the Gin4 kinase. J Cell Biol 138, 119–130.

Amon A, Tyers M, Futcher B, Nasmyth K (1993). Mechanisms that help the yeast cell cycle clock tick: G2 cyclins transcriptionally activate G2 cyclins and repress G1 cyclins. Cell 74, 993–1007.

Anderson CW, Baum PR, Gesteland RF (1973). Processing of adenovirus 2-induced proteins. J Virol 12, 241–252.

Asano S, Park JE, Sakchaisri K, Yu LR, Song S, Supavilai P, Veenstra TD, Lee KS (2005). Concerted mechanism of Swe1/Wee1 regulation by multiple kinases in budding yeast. EMBO J 24, 2194–2204.

Bi E, Pringle JR (1996). ZDS1 and ZDS2, genes whose products may regulate Cdc42p in Saccharomyces cerevisiae. Mol Cell Biol 16, 5264–5275.

Bishop AC *et al.* (2000). A chemical switch for inhibitor-sensitive alleles of any protein kinase. Nature 407, 395–401.

Booher RN, Deshaies RJ, Kirschner MW (1993). Properties of Saccharomyces cerevisiae wee1 and its differential regulation of $p34^{CDC28}$ in response to G1 and G2 cyclins. EMBO J 12, 3417–3426.

Carroll C, Altman R, Schieltz D, Yates J, Kellogg DR (1998). The septins are required for the mitosis-specific activation of the Gin4 kinase. J Cell Biol 143, 709–717.

Castilho PV, Williams BC, Mochida S, Zhao Y, Goldberg ML (2009). The M phase kinase Greatwall (Gwl) promotes inactivation of PP2A/B55{delta}, a phosphatase directed against CDK phosphosites. Mol Biol Cell 20, 4777–4789.

Clarke PR, Hoffmann I, Draetta G, Karsenti E (1993). Dephosphorylation of cdc25-C by a type-2A protein phosphatase: specific regulation during the cell cycle in Xenopus egg extracts. Mol Biol Cell 4, 397–411.

Collins SR, Kemmeren P, Zhao XC, Greenblatt JF, Spencer F, Holstege FC, Weissman JS, Krogan NJ (2007). Toward a comprehensive atlas of the physical interactome of Saccharomyces cerevisiae. Mol Cell Proteomics 6, 439–450.

Deibler RW, Kirschner MW (2010). Quantitative reconstitution of mitotic CDK1 activation in somatic cell extracts. Mol Cell 37, 753–767.

Egelhofer TA, Villen J, McCusker D, Gygi SP, Kellogg DR (2008). The septins function in G1 pathways that influence the pattern of cell growth in budding yeast. PLoS ONE 3, e2022.
Eng JK, McCormack AL, Yates JR 3rd (1994). An approach to correlate tandem mass spectral data of peptides with amino acid sequences in a protein database. J Am Soc Mass Spectrom 5, 976–989.
Evans DRH, Stark MJR (1997). Mutations in the Saccharomyces cerevisiae type 2A protein phosphatase catalytic subunit reveal roles in cell wall integrity, actin cytoskeleton organization and mitosis. Genetics 145, 227–241.
Fantes P, Nurse P (1977). Control of cell size in fission yeast by a growth modulated size control over nuclear division. Exp Cell Res 107, 377–386.
Ferrell JE, Jr (1996). Tripping the switch fantastic: how a protein kinase cascade can convert graded inputs into switch-like outputs. Trends Biochem Sci 21, 460–466.
Fitch I, Dahmann C, Surana U, Amon A, Nasmyth K, Goetsch L, Byers B, Futcher B (1992). Characterization of four B-type cyclin genes of the budding yeast *Saccharomyces cerevisiae*. Mol Biol Cell 3, 805–818.
Gachet Y, Tournier S, Millar JB, Hyams JS (2001). A MAP kinase-dependent actin checkpoint ensures proper spindle orientation in fission yeast. Nature 412, 352–355.
Gatlin GL, Kleemann GR, Hays LG, Link AJ, Yates JR (1998). Protein identification at the low femtomole level from silver-stained gels using a new fritless electrospray interface for liquid chromatography-microspray and nanospray mass spectrometry. Anal Biochem 263, 93–101.
Gautier J, Solomon MJ, Booher RN, Bazan JF, Kirschner MW (1991). cdc25 is a specific tyrosine phosphatase that directly activates p34cdc2. Cell 67, 197–211.
Gavin AC *et al*. (2002). Functional organization of the yeast proteome by systematic analysis of protein complexes. Nature 415, 141–147.
Gentry MS, Hallberg RL (2002). Localization of Saccharomyces cerevisiae protein phosphatase 2A subunits throughout mitotic cell cycle. Mol Biol Cell 13, 3477–3492.
Goldbeter A, Koshland DE, Jr (1981). An amplified sensitivity arising from covalent modification in biological systems. Proc Natl Acad Sci USA 78, 6840–6844.
Goldbeter A, Koshland DE, Jr (1984). Ultrasensitivity in biochemical systems controlled by covalent modification. Interplay between zero-order and multistep effects. J Biol Chem 259, 14441–14447.
Harvey SL, Charlet A, Haas W, Gygi SP, Kellogg DR (2005). Cdk1-dependent regulation of the mitotic inhibitor Wee1. Cell 122, 407–420.
Harvey SL, Kellogg DR (2003). Conservation of mechanisms controlling entry into mitosis: budding yeast wee1 delays entry into mitosis and is required for cell size control. Curr Biol 13, 264–275.
Healy AM, Zolnierowicz S, Stapleton AE, Goebl M, DePaoli-Roach AA, Pringle JR (1991). Cdc55, a *Saccharomyces cerevisiae* gene involved in cellular morphogenesis: identification, characterization, homology to the B subunit of mammalian type 2A protein phosphatase. Mol Cell Biol 11, 5767–5780.
Hoffman I, Clarke PR, Marcote MJ, Karsenti E, Draetta G (1993). Phosphorylation and activation of human cdc25-C by cdc2-cyclin B and its involvement in the self amplification of MPF at mitosis. EMBO J 12, 53–63.
Izumi T, Maller JL (1993). Elimination of cdc2 phosphorylation sites in the cdc25 phosphatase blocks initiation of M-phase. Mol Biol Cell 12, 1337–1350.
Izumi T, Maller JL (1995). Phosphorylation and activation of the Xenopus Cdc25 phosphatase in the absence of Cdc2 and Cdk2 kinase activity. Mol Biol Cell 6, 215–216.
Izumi T, Walker DH, Maller JL (1992). Periodic changes in the phosphorylation of the Xenopus Cdc25 phosphatase regulate its activity. Mol Biol Cell 3, 927–939.
Janssens V, Goris J (2001). Protein phosphatase 2A: a highly regulated family of serine/threonine phosphatases implicated in cell growth and signalling. Biochem J 353, 417–439.
Jorgensen P, Nishikawa JL, Breitkreutz BJ, Tyers M (2002). Systematic identification of pathways that couple cell growth and division in yeast. Science 297, 395–400.
Kellogg DR (2003). Wee1-dependent mechanisms required for coordination of cell growth and cell division. J Cell Sci 116, 4883–4890.
Kellogg DR, Alberts BM (1992). Purification of a multiprotein complex containing centrosomal proteins from the Drosophila embryo by chromatography with low-affinity polyclonal antibodies. Mol Biol Cell 3, 1–11.
Kumagai A, Dunphy WG (1991). The cdc25 protein controls tyrosine dephosphorylation of the cdc2 protein in a cell-free system. Cell 64, 903–914.
Kumagai A, Dunphy WG (1992). Regulation of the cdc25 protein during the cell cycle in Xenopus extracts. Cell 70, 139–151.
Lew D, Reed SI (1995). A cell cycle checkpoint monitors cell morphogenesis in budding yeast. J Cell Biol 129, 739–749.
Lew DJ (2003). The morphogenesis checkpoint: how yeast cells watch their figures. Curr Opin Cell Biol 15, 648–653.
Lew DJ, Reed SI (1993). Morphogenesis in the yeast cell cycle: regulation by Cdc28 and cyclins. J Cell Biol 120, 1305–1320.
Lin FC, Arndt KT (1995). The role of *Saccharomyces cerevisiae* type 2A phosphatase in the actin cytoskeleton and in entry into mitosis. EMBO J 14, 2745–2759.
Longtine MS, McKenzie A, DeMarini D, Shah NG, Wach A, Brachat A, Philippsen P, Pringle JR (1998). Additional modules for versatile and economical PCR-based gene deletion and modification in Saccharomyces cerevisiae. Yeast 14, 953–961.
Longtine MS, Theesfeld CL, McMillan JN, Weaver E, Pringle JR, Lew DJ (2000). Septin-dependent assembly of a cell cycle-regulatory module in Saccharomyces cerevisiae. Mol Cell Biol 20, 4049–4061.
Ma XJ, Lu Q, Grunstein M (1996). A search for proteins that interact genetically with histone H3 and H4 amino termini uncovers novel regulators of the Swe1 kinase in Saccharomyces cerevisiae. Genes Dev 10, 1327–1340.
McCusker D, Denison C, Anderson S, Egelhofer TA, Yates JR, 3rd, Gygi SP, Kellogg DR (2007). Cdk1 coordinates cell-surface growth with the cell cycle. Nat Cell Biol 9, 506–515.
McMillan JN, Sia RAL, Bardes SG, Lew DJ (1999). Phosphorylation-independent inhibition of Cdc28p by the tyrosine kinase Swe1p in the morphogenesis checkpoint. Mol Cell Biol 19, 5981–5990.
McMillan JN, Sia RAL, Lew DJ (1998). A morphogenesis checkpoint monitors the actin cytoskeleton in yeast. J Cell Biol 142, 1487–1499.
Minshull J, Straight A, Rudner AD, Dernburg AF, Belmont A, Murray AW (1996). Protein phosphatase 2A regulates MPF activity and sister chromatid cohesion in budding yeast. Curr Biol 6, 1609–1620.
Mochida S, Ikeo S, Gannon J, Hunt T (2009). Regulated activity of PP2A-B55 delta is crucial for controlling entry into and exit from mitosis in Xenopus egg extracts. EMBO J 28, 2777–2785.
Morgan DO (2007). The Cell Cycle: Principles of Control, New Science Press Ltd.
Mueller PR, Coleman TR, Dunphy WG (1995). Cell cycle regulation of a Xenopus Wee1-like kinase. Mol Biol Cell 6, 119–134.
Nurse P (1975). Genetic control of cell size at cell division in yeast. Nature 256, 547–551.
Nurse P, Thuriaux P, Nasmyth K (1976). Genetic control of the cell division cycle in the fission yeast *Schizosaccharomyces pombe*. Mol Gen Genet 146, 167–178.
Pal G, Paraz MT, Kellogg DR (2008). Regulation of Mih1/Cdc25 by protein phosphatase 2A and casein kinase 1. J Cell Biol 180, 931–945.
Perry JA, Kornbluth S (2007). Cdc25 and Wee1: analogous opposites? Cell Div 2, 12.
Pringle JR, Adams AEM, Drubin DG, Haarer BK (1991). Immunofluorescence methods for yeast. Methods Enzymol 194, 565–602.
Queralt E, Lehane C, Novak B, Uhlmann F (2006). Downregulation of PP2A(Cdc55) phosphatase by separase initiates mitotic exit in budding yeast. Cell 125, 719–732.
Queralt E, Uhlmann F (2008). Separase cooperates with Zds1 and Zds2 to activate Cdc14 phosphatase in early anaphase. J Cell Biol 182, 873–883.
Rahal R, Amon A (2008). Mitotic CDKs control the metaphase-anaphase transition and trigger spindle elongation. Genes Dev 22, 1534–1548.
Reinhardt HC, Yaffe MB (2009). Kinases that control the cell cycle in response to DNA damage: Chk1, Chk2, MK2. Curr Opin Cell Biol 21, 245–255.
Robinson LC *et al*. (1992). Yeast casein kinase I homologues: an essential gene pair. Proc Natl Acad Sci USA 89, 28 32.
Robinson LC, Menold MM, Garrett S, Culbertson MR (1993). Casein kinase I-like protein kinases encoded by YCK1 and YCK2 are required for yeast morphogenesis. Mol Cell Biol 13, 2870–2881.
Rupes I (2002). Checking cell size in yeast. Trends Genet 18, 479 485.
Rupes I, Webb BA, Mak A, Young PG (2001) G2/M arrest caused by actin disruption is a manifestation of the cell size checkpoint in fission yeast. Mol Biol Cell 12, 3892–3903.
Russell P, Moreno S, Reed SI (1989). Conservation of mitotic controls in fission and budding yeasts. Cell 57, 295 303.
Russell P, Nurse P (1986). cdc25+ functions as an inducer in the mitotic control of fission yeast. Cell 45, 145–153.
Russell P, Nurse P (1987). Negative regulation of mitosis by wee1+, a gene encoding a protein kinase homolog. Cell 49, 559–567.

Schwob E, Nasmyth K (1993). CLB5 and CLB6, a new pair of B cyclins involved in DNA replication in *Saccharomyces cerevisae*. Genes Dev 7, 1160–1175.
Shulewitz MJ, Inouye CJ, Thorner J (1999). Hsl7 localizes to a septin ring and serves as an adapter in regulatory pathway that relieves tyrosine phosphorylation of Cdc28 protein kinase in Saccharomyces cerevisiae. Mol Cell Biol 19, 7123–7137.
Sreenivasan A, Kellogg D (1999). The Elm1 kinase functions in a mitotic signaling network in budding yeast. Mol Cell Biol 19, 7983–7994.
Stark MJR (1996). Yeast protein serine/threonine phosphatases: multiple roles and diverse regulation. Yeast 12, 1647–1675.
Surana U, Robitsch H, Price C, Schuster T, Fitch I, Futcher AB, Nasmyth K (1991). The role of CDC28 and cyclins during mitosis in the budding yeast S. cerevisiae. Cell 65, 145–161.
Tang Z, Coleman TR, Dunphy WG (1993). Two distinct mechanisms for negative regulation of the Wee1 protein kinase. EMBO J 12, 3427–3436.
Theesfeld CL, Irazoqui JE, Bloom K, Lew DJ (1999). The role of actin in spindle orientation changes during the Saccharomyces cerevisiae cell cycle. J Cell Biol 146, 1019–1032.
Trinkle-Mulcahy L, Lamond AI (2006). Mitotic phosphatases: no longer silent partners. Curr Opin Cell Biol 18, 623–631.
Wang Z, Kar S, Carr BI (2008). Cdc25A protein phosphatase: a therapeutic target for liver cancer therapies. Anticancer Agents Med Chem 8, 863–871.
Wilm M, Shevchenko T, Houthaeve T, Breit S, Schweigerer L, Fotsis T, Mann M (1996). Femtomole sequencing of proteins from polyacrylamide gels by nano-electrospray mass spectrometry. Nature 379, 466–499.
Wu L, Russell P (1993). Nim1 kinase promotes mitosis by inactivating Wee1 tyrosine kinase. Nature 363, 738–741.
Yang H, Jiang W, Gentry M, Hallberg RL (2000). Loss of a protein phosphatase 2A regulatory subunit (Cdc55p) elicits improper regulation of Swe1p degradation. Mol Cell Biol 20, 8143–8156.
Yasutis K, Vignali M, Ryder M, Tameire F, Dighe SA, Fields S, Kozminski KG (2010). Zds2p regulates Swe1p-dependent polarized cell growth in Saccharomyces cerevisiae via a novel Cdc55p interaction domain. Mol Biol Cell 21, (*in press*).
Yu Y, Jiang YW, Wellinger RJ, Carlson K, Roberts JM, Stillman DJ (1996). Mutations in the homologous ZDS1 and ZDS2 genes affect cell cycle progression. Mol Cell Biol 16, 5254–5263.
Zhao Y, Boguslawski G, Zitomer RS, DePaoli-Roach AA (1997). Saccharomyces cerevisiae homologs of mammalian B and B′ subunits of protein phosphatase 2A direct the enzyme to distinct cellular functions. J Biol Chem 272, 8256–8262.